

# Scientific report for the field work conducted in October 2007, Gelai area - northern Tanzania

Damien Delvaux, Benoît Smets, Christelle Wauthier, Athanas S. Macheyekei

Tervuren, January 2008

## Introduction

A seismic crisis with a series of moderate earthquakes started on July 12<sup>th</sup> 2007 in the Lake Natron area in North Tanzania. According to the USGS - NEIC earthquake catalogue, it lasted on the 8<sup>th</sup> of September 2007, where 80 teleseismic earthquakes were recorded, with the strongest one on the 17<sup>th</sup> July at 14hr10min GMT. For the same period, 6 focal mechanisms were provided by the Harvard CMT catalogue.

Soon after the main event of July 17<sup>th</sup>, R. Ferdinand from the University of Dar Es Salaam and E. Sariah from Arthi University visited the site and reported the presence of important surface fissures on the ground, but without mapping them in detail. They also re - measured the Engaresero GPS site and installed seismic stations at Engaresero and Gelai villages.

Within the frame of the ongoing SAAMAV project, several SAR images (from ENVISAT satellite, descending orbit) were acquired and processed by Nicolas d'Oreye of the National Institute for Natural History, Luxemburg and his team. They obtained interferograms that show the presence of two fault systems delimiting a NNE - trending narrow graben in the southern flank of the Gelai Mountain. After preliminary modelling, Eric Calais and Nicolas d'Oreye, suggested that the structures observed on the interferograms could be best interpreted in a sequence of deformations involving the emplacement of a subvertical dike at depth under the graben structure.

Therefore, in October 2007, the Royal Museum for Central Africa organised a field campaign in order to collect field data in order to constrain the preliminary interpretations based on the SAR interferometry images and to describe and map the surface fissures related to the July - August volcano - tectonic event. The field campaign was organised thanks to the help of E. Sariah from the Department of Geomatics of the ARDHI University of Dar es Salaam (formerly UCLAS), with the logistic help of the Ministry of Land Survey and the participation of A.S. Macheyekei, geologist and Ph.D Student from the Madini Institute (Dodoma, Tanzania) and Ghent University (Belgium).

The two main objectives for this field campaign were (1) to map the surface fissures related to the July - August volcano - tectonic event, (2) record the volcanic activity of the Oldoinyo Lengai volcano and (3) to re - measure the Engaruka GPS site, to install and measure additional GPS points across the faulted structures. This report concerns objective one, i.e. mapping of surface fissures.

## **Field mapping**

The target for field mapping was first based on the preliminary observations of fault segments made by R. Ferdinand and E. Sariah in July 2007, soon after the main seismic event. The structures as revealed by the SAR interferograms were of great help in the field when tracking the discontinuous and overlapping of the fault segments, even though some fault segments north of Gelai were accidentally discovered towards the end of the field mission.

Priority was given to the mapping of the surface fractures as detailed as possible. Measurements of the associated deformation were made using a metric tape. The morphology, orientation and arrangement of the fractures, together with their geological and morphological contexts were also described. Evidences for reactivation of older fracture systems were noted. Other field parameters were illustrated using both digital and argentic (slides) photography's. The coordinates of the observation points were recorded using a Garmin eTrex hand GPS, regularly downloaded on a Laptop computer.

In addition to the systematic mapping, a few topographic profiles across the graben structure were made using a Leica System 1200 Differential GPS.

## **GIS - data integration**

Using 1:125,000 topographic maps and 1:250,000 geological maps scanned and referenced earlier by François Kervyn, a GIS Database was created on Mapinfo. During the field campaign, air photographs of the Gelai – Oldoinyo Lengai area were obtained at the Land Survey Department in Dar es Salaam. The air photographs were geo – referenced; with the topographic maps as a basis. To do this, about 100 - 200 common control points were used. The mean error for each geo - referenced air photograph was kept about 30 – 40 m. However, it has to be noted that for technical reasons, it was not possible to orthorectify the air photographs before the referencing them.

The SRTM - data were also used to produce the corresponding digital elevation model (DEM) and colour - coded shaded topographic maps.

## **Results**

### **Map of observed fissures**

The surface fractures (fault segments) are plotted on Figure 1. In the field, the fractures often appear as a series of relatively small segments, arranged in an en-échelon pattern; some are left overstepping and others are right overstepping. In places where fault segments are more than a few meter long, they were mapped as polylines otherwise they were mapped as isolated GPS points.

On the western side of the deformed zone only one fracture system was mapped, while five different fracture systems were identified on the eastern side (E1 - 4). They were further subdivided into segments according to their field characteristics: segments W-1, W-2, W-3 for the western fracture system, and segments E1-1, E1-2, E1-3, E2-1, E2-2, E2-3, E2-4, E3, E4 and E5 for the eastern fracture system (Figure 2). The western fracture system has not been mapped entirely due to limited time and accessibility problems, but field relationship show that it most likely continues further to the north.

The surface fractures observed are commonly subvertical at the surface. Along segment E1-2, vertical depth of 8.5 m was obtained. Generally, the fractures appear as open tension cracks of limited lateral extent, with a general en-échelon arrangement ranging from metric to kilometric scale. Both horizontal opening (dilation) and vertical offset are at the scale of few centimetres to few decimetres. Field relationship shows that with exception of segment E1-3, the vertical down - faulting along the western fault system is on the eastern side whereas along the eastern fault system, it is on the western side. In that case, the portion of land enclosed between the two fracture systems defines a central graben (Figure 2).

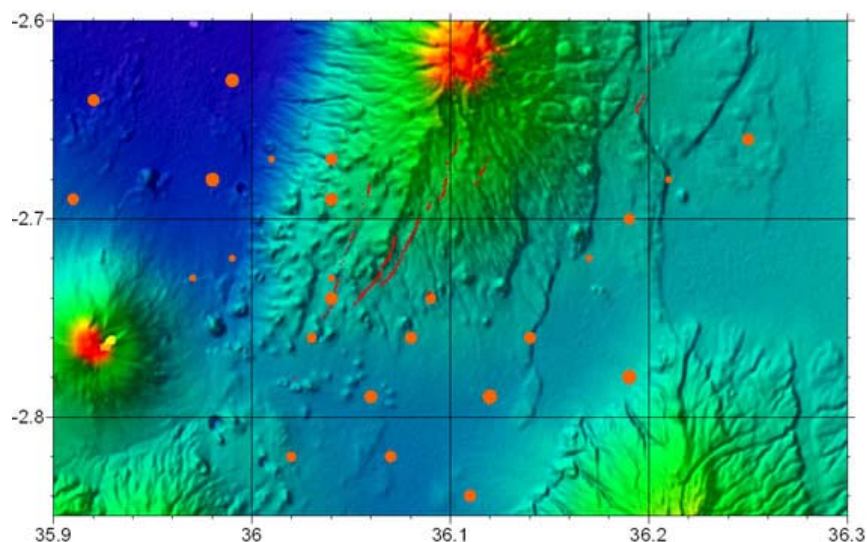


Figure 1. General overview of the mapped fractures (red lines and dots) on the background of colour - coded shaded - relief image of the SRTM - DEM at 90 m resolution. Orange dots correspond to the seismic epicentres from the July - August 2007 seismic crisis, relocated by Julie Albaric (preliminary data only). Note that the strongest event of the sequence (July 17, Mw 5.9) is located outside the map, just east of it. Geodetic coordinates in degrees, WGS84 datum,  $0.1^\circ$  corresponding to 9 km.

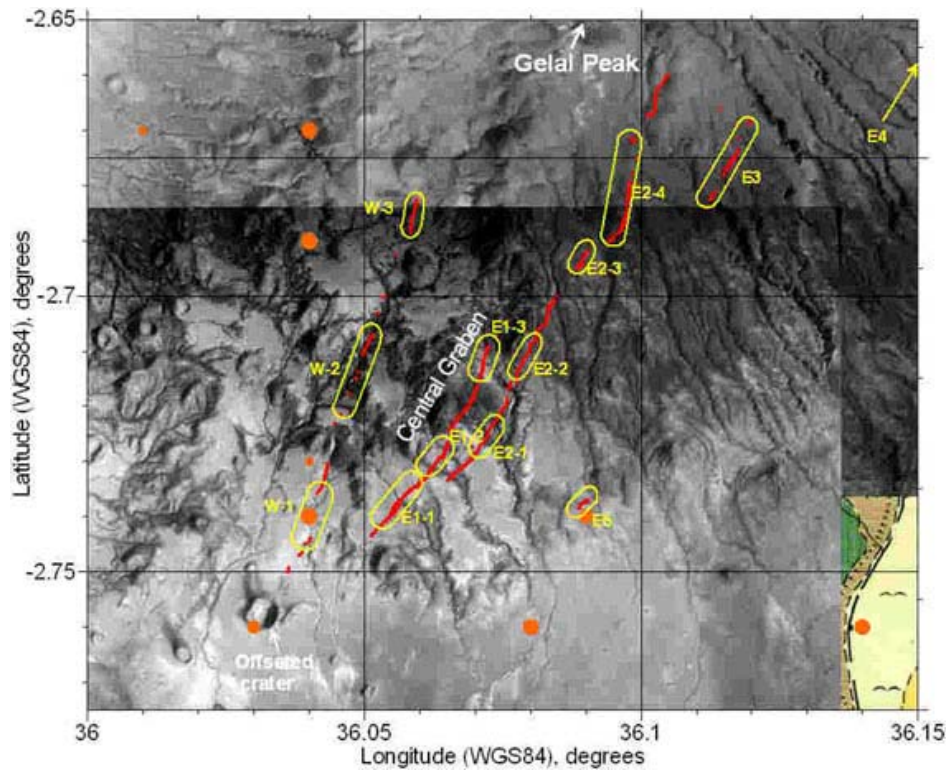


Figure 2. Closer view of the mapped fractures (red lines and dots) on the background of geo - referenced air photographs. The encircled data and labels in yellow correspond to the fault segments for which the average values of displacement are reported in Table 1. Segment E4 located on the northeastern extremity of the mapped structure is outside the limits of the map (see Figure 1). The expected Gelai tectono - magmatic graben is located between the western and the eastern fault systems. Geodetic coordinates in degrees, WGS84 datum,  $0.05^\circ$  corresponding to 4.5 km.

The mapped surface fractures correspond fairly well with fringe discontinuities of the interferogram spanning the main earthquake of July 17<sup>th</sup> (Figure 3). The fringe discontinuities, however, extend laterally further than the open fractures observed in the field. Part of this apparent mismatch is due to incomplete observation in the field as for the northern portion of the western fracture system which could not be mapped. It is possible also that isolated or weakly expressed fractures were missed in the area mapped. The remaining part of the mismatch might indicate subsurface deformation without opening of visible tension fractures at the surface, but rather with discrete and / or diffuse zone of extension.

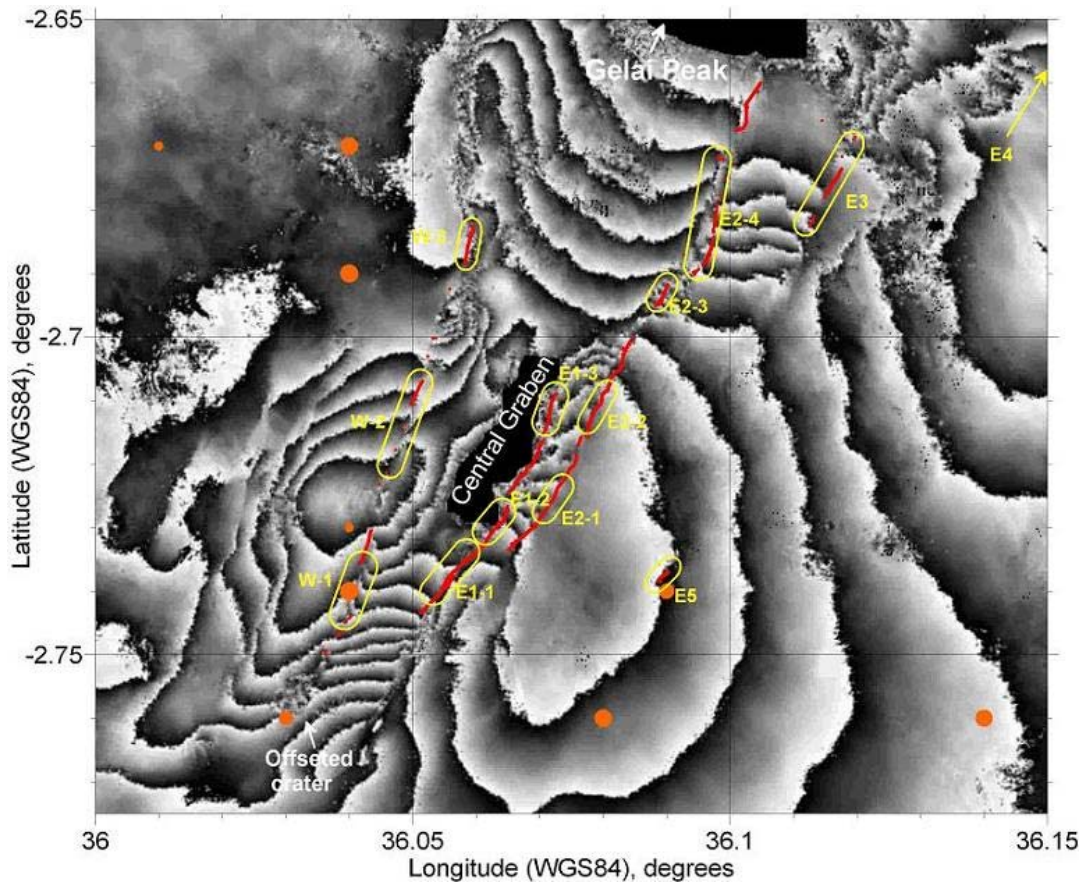


Figure 3. Plot of the fracture systems on an interferogram spanning the main earthquake of July 17<sup>th</sup> (Courtesy Nicolas d'Oreye). The mapped ruptures (in red) correspond well with the fringe discontinuities, although the latter seem to extend laterally over a longer distance than the observed surface ruptures. Orange dots correspond to the seismic epicentres from the July-August 2007 seismic crisis, relocated by Julie Albaric (preliminary data only). Geodetic coordinates in degrees, WGS84 datum, 0.05° corresponding to 4.5 km.

Figure 4 shows that fault E2 is developed at the foot of a multi - event morphological scarp and on older ruptures highlighted on the air photographs by a line of darker vegetation. The 2007 surface ruptures seem to follow such old scarps.

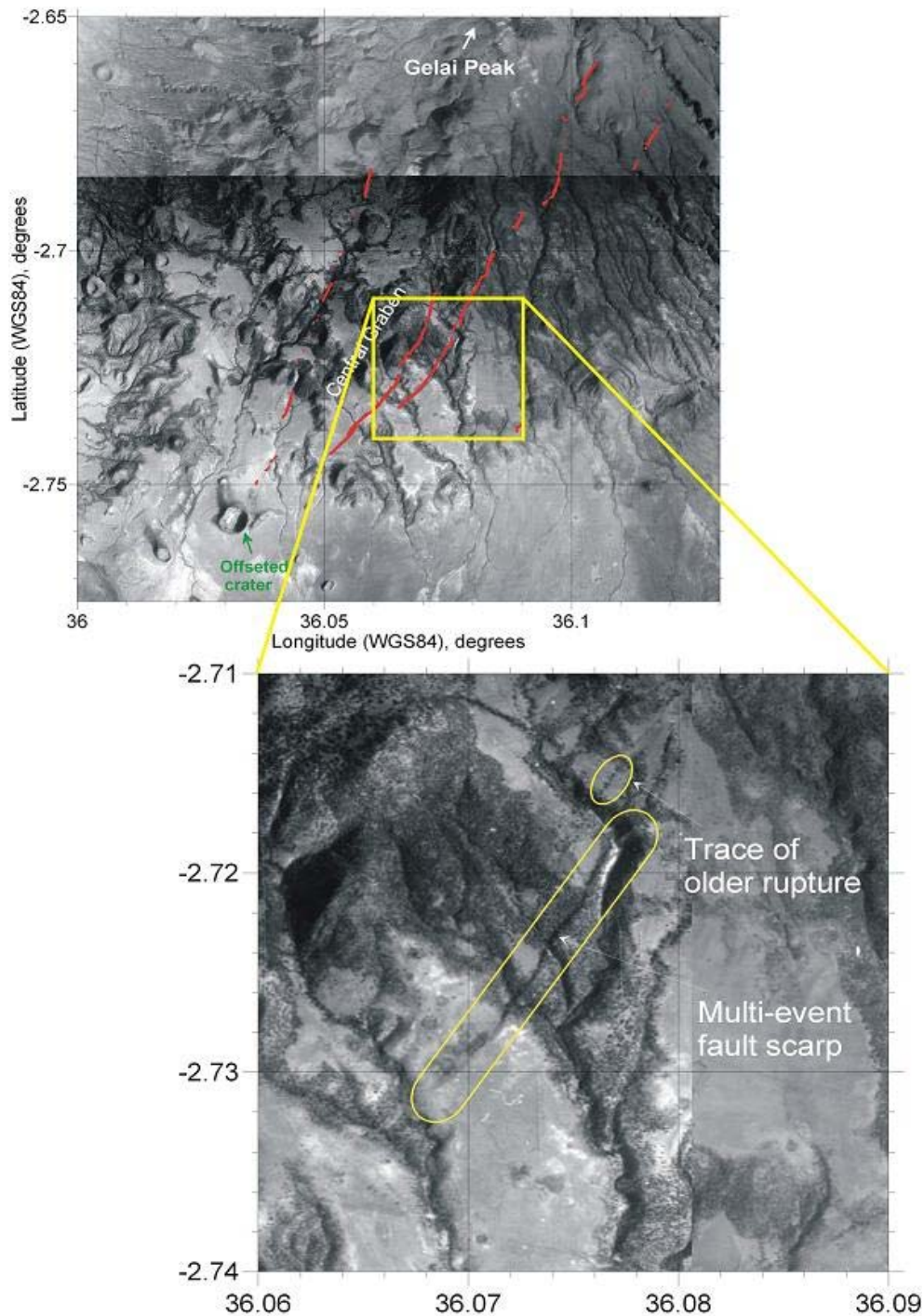


Figure 4. Detail of the relay between the two eastern faults delimiting the graben. According to field observations and air photographs - interpretation, the fractures E2 seem to correspond to reactivation of older faults / and ruptures. Geodetic coordinates are in degrees, WGS84 datum,  $0.01^\circ$  corresponding to 900 m.

The two fault systems seem to converge towards the southwestern direction, thus progressively narrowing the central graben. If the lines of the observed surface fractures are extrapolated south - westwards, they join in the middle of a morphologically fresh volcanic crater characterized by pyroclastic deposits (Figure 5). In further detail (Figure 6), the rim of

this crater is cut and displaced at two points by a recent fault which is interpreted to be a southwards prolongation of the western fault system. A rapid field check confirms that the fractures affecting the crater rim are subvertical, with down - thrown block due east. No fresh fractures related to the July - August 2007 event could be observed however.

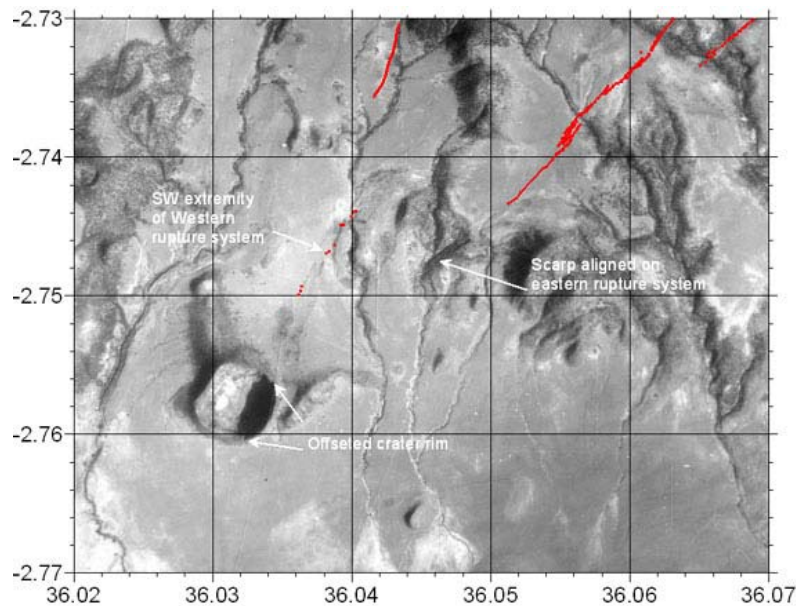


Figure 5. Detail of the southwestern closure of the fault graben enclosed between the Western fault (center - north of the map) and the Eastern fault system (NE corner of the map). The two fault systems apparently continue southwestwards further than the last surface fractures opened during the July - August event are observed. They seem to intersect at the location of a rounded crater whose rim is offset by a recent fault at two locations. Geodetic coordinates in degrees, WGS84 datum:  $0.01^\circ$  corresponding to 900 m.

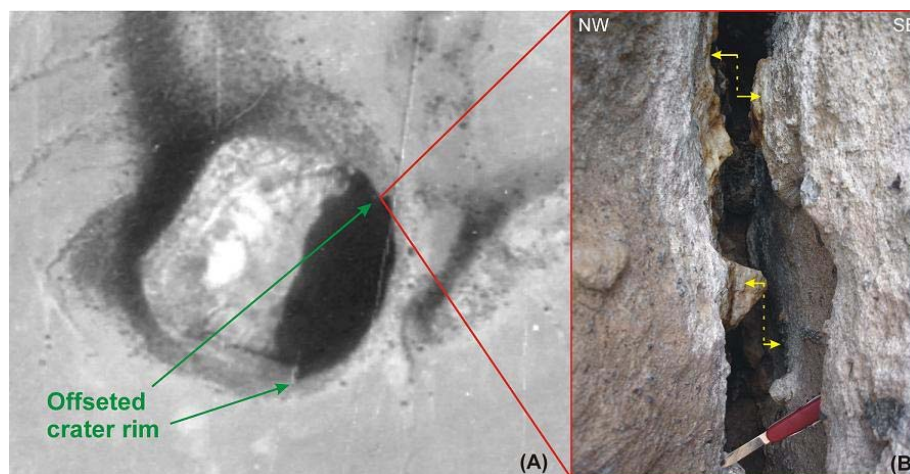


Figure 6. (A) Zoom on Figure 5, corresponding to the crater area. The crater rim seem to be offset by a recent fault at two locations. (B) Details of an older fissure in the northeastern corner of crater rim. The vertical offset is about 5 cm.

**Displacement profiles**

As highlighted earlier, apart from the mapping of the surface fractures, measurements of both horizontal opening or dilation ( $\Delta h$ ) and vertical offset ( $\Delta v$ ) were undertaken taking into account of the possibilities for fracture margins collapse (s). To illustrate the variation of the dilation and vertical offsets along the fault systems, the Displacement Profiles were constructed in order to show the horizontal opening and vertical offset versus distance along the faults, using the southernmost observation points as points of origin (Figures 7 & 8).

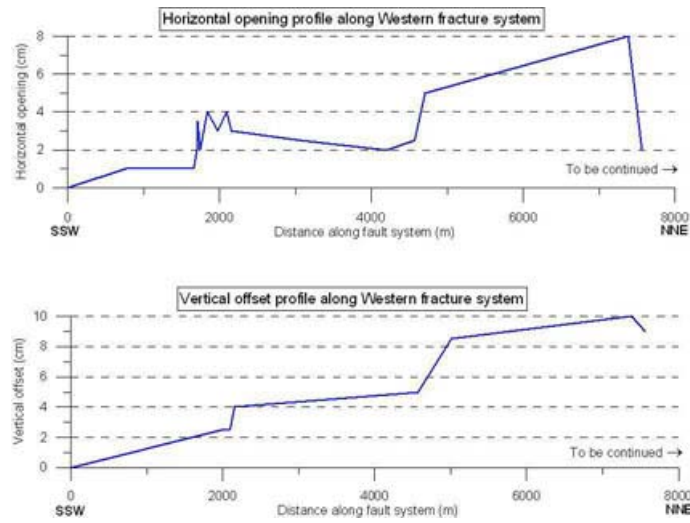


Figure 7. Displacement profiles for the western fracture system W1, showing the horizontal opening ( $\Delta h$ ) and vertical offset ( $\Delta v$ ) versus distance along the fault, point of origin being at the southwestern side of the fault. Note that only the southern part of the western fracture system has been mapped (vertical offset is down to the East).

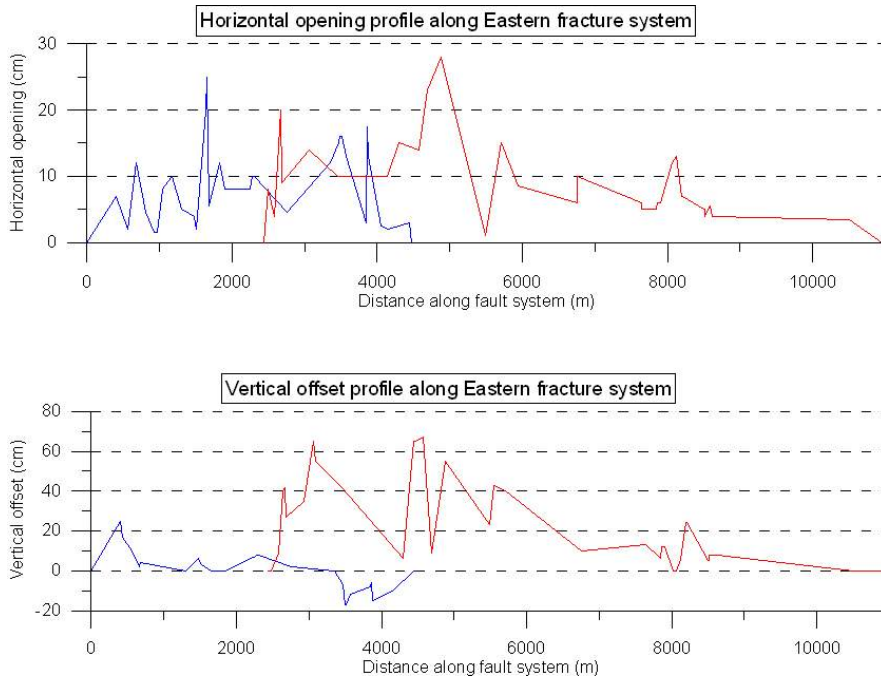


Figure 8. Displacement profiles for the eastern fracture system. Blue lines and red lines represent fracture E1 and fracture E2 respectively. Vertical and horizontal scales as in Figure 7. When the down – thrown block is down due west it is positive and negative when down – thrown due east.

### Average displacement parameters

As can be seen from the displacement profiles (Figures 7 & 8), the values of  $\Delta h$  and  $\Delta v$  are rapidly fluctuating along trend. This is probably due to the highly segmented and sometimes discontinuous nature of the fractures. Moreover, it was not always possible to measure these values due to local outcrop conditions. Therefore, instead the values were averaged for the different segments as reported in Table 1. For each segment, the number of measurements made, the average, minimal and maximal values for  $\Delta h$  and  $\Delta v$  are presented.

Most average values of  $\Delta h$  as  $\Delta v$  are within a centimetre scale, with the smallest values for the western segment. The largest values are observed on fault E2, especially along its southernmost segments E2-1 and E2-2. The segments respectively show average of  $\Delta h$  of  $10.8 \pm 5.5$  and  $14.3 \pm 8.4$  cm with maximum measured values of 20 and 28 cm. Their vertical  $\Delta v$  offsets are respectively  $31.5 \pm 22.3$  cm and  $41.3 \pm 22.6$  cm, with maxima at 65 cm for both segments. The average values have in general high standard deviation, reflecting probably the segmented and discontinuous character of the fractures. For all the fractures observed, no significant lateral displacement could be measured.

### Open fracture – normal fault relationship

The frequently observed combination of horizontal opening and vertical offset associated with the subvertical fractures observed at the surface can be explained using the typical geometry of fracture systems that have been evidenced in northern Iceland by Angelier et al. (1997).

They established a geometrical and genetic relationship between subvertical tension fractures at the surface and shear faults with dips between  $60$  and  $75^\circ$  at depths (Figure. 9). In the absence of strike - slip movements, which seems the case also here, they evidence an approximately linear relationship between  $\Delta h$  and  $\Delta v$  for a large number of surface fractures measured. Based on this relationship and combining structural observations at different structural levels, they propose a model in which the open subvertical fractures near the surface change abruptly into normal faults dipping  $60$ - $72^\circ$  at moderate depth. Therefore, combining the  $\Delta h$  and  $\Delta v$  values of a given fracture observed at subsurface, one can obtain the dip - angle of the underlying fault and the associated net slip. In the present case, the dip angle and net slips were computed on the average values of  $\Delta h$  and  $\Delta v$  for each segments when possible (Table 1, last two columns).

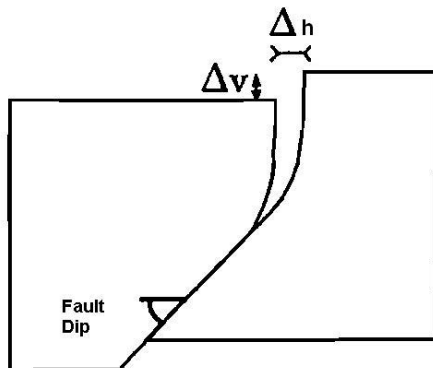


Figure 9....., Figure 90, from Angelier et al. (1997).

$$\text{Fault Dip} = \text{Arctan} (\Delta v / \Delta h)$$

$$\text{Net Slip} = \text{Sqrt} (\Delta v^2 + \Delta h^2)$$

It is interesting to notice that the values obtained generally fall between  $60$  and  $72^\circ$  as observed in their work of Angelier et al. (1997). The rather low angle obtained for segment

E1-2 (22.5°) is not considered to be significant as it forms the transition between the west - dipping E1-1 segment and the east - dipping E1-3 segment.

The nature of the transition between the vertical surface fissures and the normal faults at depth is subject to discussion. Using structural observations, combining surface fractures and shear faults at deeper structural level, Angelier et al. (1997) concludes that an abrupt change from the open vertical fissures near the surface to normal faults at moderate depth is more likely. They also found that the most frequent dip angle of these normal faults are between 60 and 72°, similarly as what is calculated here. Although they could not investigate directly the depth of transition between the vertical fissures and the normal faults, Angelier et al (1997) observed that the extensional deformation at paleodepths of 1-2 km is dominantly accommodated by normal faulting. They also suggest that at mid crustal depth (2-5 km), effective tension mechanism plays an important role, through magmatic injection.

### **Listric versus planar fault at depth and reactivations**

A differential GPS profile was measured across segment 1 of the eastern fracture system E1, where the July 2007 fissures appeared at the base of the existing morphological scarp visible on Figure 4 (details of profile in Figure 10). The red and blue lines represent the fits to the planar portions of the topographic surface which have been displaced by repeated faulting events. Unfortunately, the topographic profile was not measured far enough to the SE (to the right on the figure). In spite of that, the slope difference between the two surfaces is less than 1 ° (0.86°). Should the profile be continued more to the right, probably a close parallelism would be obtained. This suggests that no component of block rotation is involved in the long - term faulting and that the fault profile at depth should be straight and not listric as would be the case if block rotation occurred. In the absence of block rotation, the vertical separation between the two surfaces represents the total vertical offset associated with the repeated faulting events along that scarp, ever since the planar topographic surfaces were formed.

In the present case, the total vertical offset calculated is 14.25 m. It should be considered as a minimum value since the upper surface slope is probably a bit underestimated because the topographic profiles were not recorded far enough western wards. According to (?), a minimum number of 45 earthquake events similar to the July 2007 one are necessary to explain this total vertical offset.

In conclusion, analysis of this profile shows that the normal fault at depth, under the transition with the vertical fracture, should be planar. In addition, the July 2007 earthquake event is just the last of a series of similar events that occurred earlier in the same area.

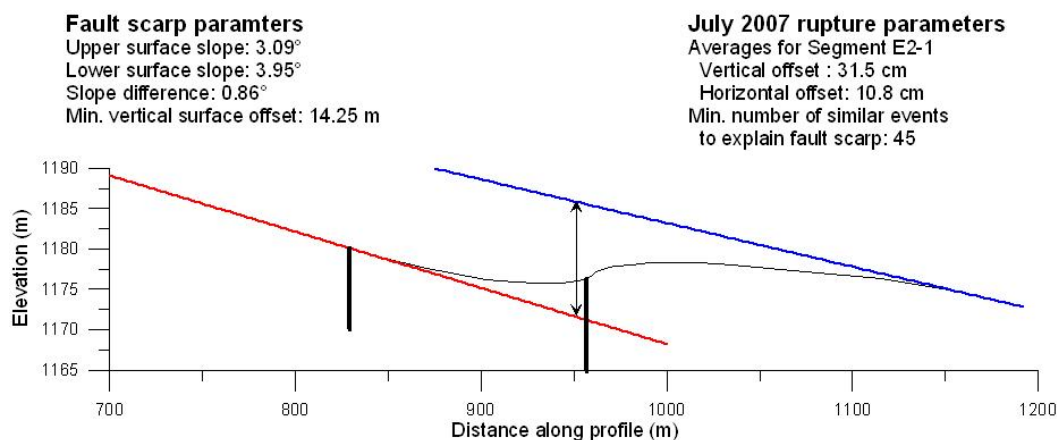


Figure 10. Detail of a differential GPS topographic profile across segment E2-1 (location on Figure 4a) showing location of the 2007 surface fissures in relation to the long-term morphological fault scarp (the main fracture on the right side).

### Constrain on the top dike geometry

In the previous paragraph, it is suggested that the observed subvertical fractures with both horizontal dilation and vertical offset are likely to reflect normal faulting with dips varying between 60 and 72° at depth. Furthermore, these fractures are aligned along two systems that show opposed sense of displacement delimiting the central graben. Extrapolation of the underlying faults at depth reaches a point where they intersect. It has been shown above that it is suspected that the July - August moderate to strong - magnitude earthquake swarm crisis might correspond to a volcano-tectonic event during which a magmatic dike emplaced at depth under the southern flank of the Gelai volcano. This scenario corresponds to the volcano-extensional structures that formed in the upper crust by vertical magma intrusion accompanied by seismicity and deformation (Hackett et al., 1996).

According to this model, the graben developing between the two convergent fault systems should be underlain by a thin subvertical dike injection. The top of this dike should approximately correspond to the intersection of the lines prolonging the two normal faults (even if physically, the faults do not join the top of dike). The downward intersection of the two fault systems should therefore represent the approximate depth of the top of the dike that caused them. Based on this, a differential GPS topographic profile was measured in the field, orthogonal to the direction of the central graben and intersecting fault segments W1 (N49°E) and E1-1 (N61°W). The calculation of the X and Y coordinates of the top of dike and its elevation Z is illustrated on Figure 11.

The coordinates of the normal fault intersection, assumed to be close to the top of dike along selected topographic sections is calculated using a model where the vertical open fractures observed at surface change sharply into shear faults whose inclination is given by the ratio between  $\Delta h$  and  $\Delta v$ . For this calculation,  $\Delta v$  of surface fractures is assumed to be 50 m for all fractures. Measurement on one point along fracture E1-2 gives a minimum value of 8.5 m for the  $\Delta v$ . Field data alone cannot constrain this parameter. Two assumptions can be made here. First, an assumption is made that the height of the vertical fractures is the same at every point. Second, the value imposed for that height should be at least 8.5 m but cannot be further

constrained. Therefore, this should be either studied in the field by geophysical means, or considered as an unknown parameter that has to be estimated by modelling.

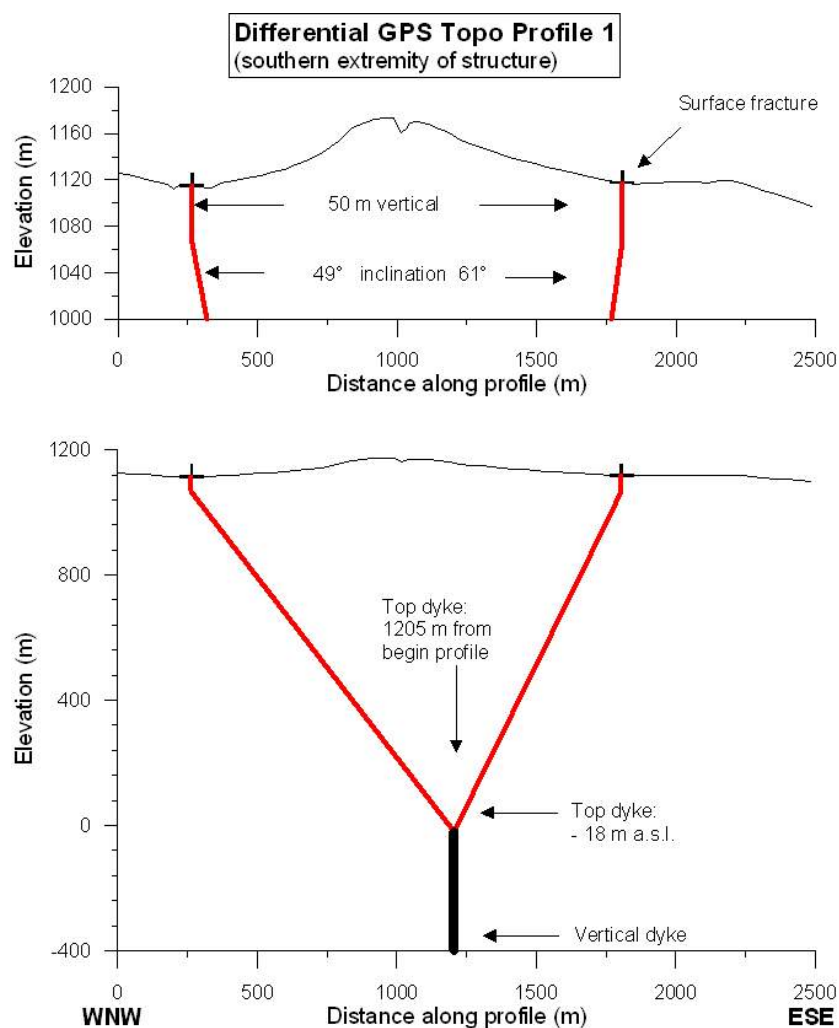


Figure 11. Differential GPS profile across the Gelai tectono - magmatic graben (close to SRTM profile 1 in Figure 11) illustrating the calculation of the position of the top of the inferred underlying dike. The crosses show the intersection of the fault segment on the profile. The fractures are drawn vertically to a depth of 50 m (see comment on this above), after which in a sharp transition, they evolve in normal faults whose slope is constrained by the average values of  $\Delta h$  and  $\Delta v$  for the respective segments. The downward projection of the two faults intersects at an elevation of -18 m and at a distance of 1205 m from the origin of the profile on its northwestern side.

In order to map the top of the dike under the central graben, a series of 6 topographic sections (Figure 12) were extracted from the SRTM DEM at a right angle to the graben axis (Figure 13). The calculated coordinates of the dike top are presented in Table 2. In plan view, the top of dike displays a curved geometry, aligned between the summits of the Gelai and the Kerimasi volcanoes (Figure 13). Our data do not allow assessing the dip angle of the dike. For the profile 5, the dip angle of the underlying normal fault along the western side of the graben is constrained not only by 2 values of  $\Delta h$  and  $\Delta v$  for the segment E2-3. Therefore, three different calculations were made, with dip values of 65°, 68° and 70°, intermediate between

the dip of  $71^\circ$  calculated for segment E2-2 (11 data) and of  $62^\circ$  obtained for segment E2-4 (18 data). From dip values of  $65$  to  $70^\circ$ , the calculated top of dike is progressively deeper, but also at a greater distance from the origin of the section, further to the SE (Table 2).

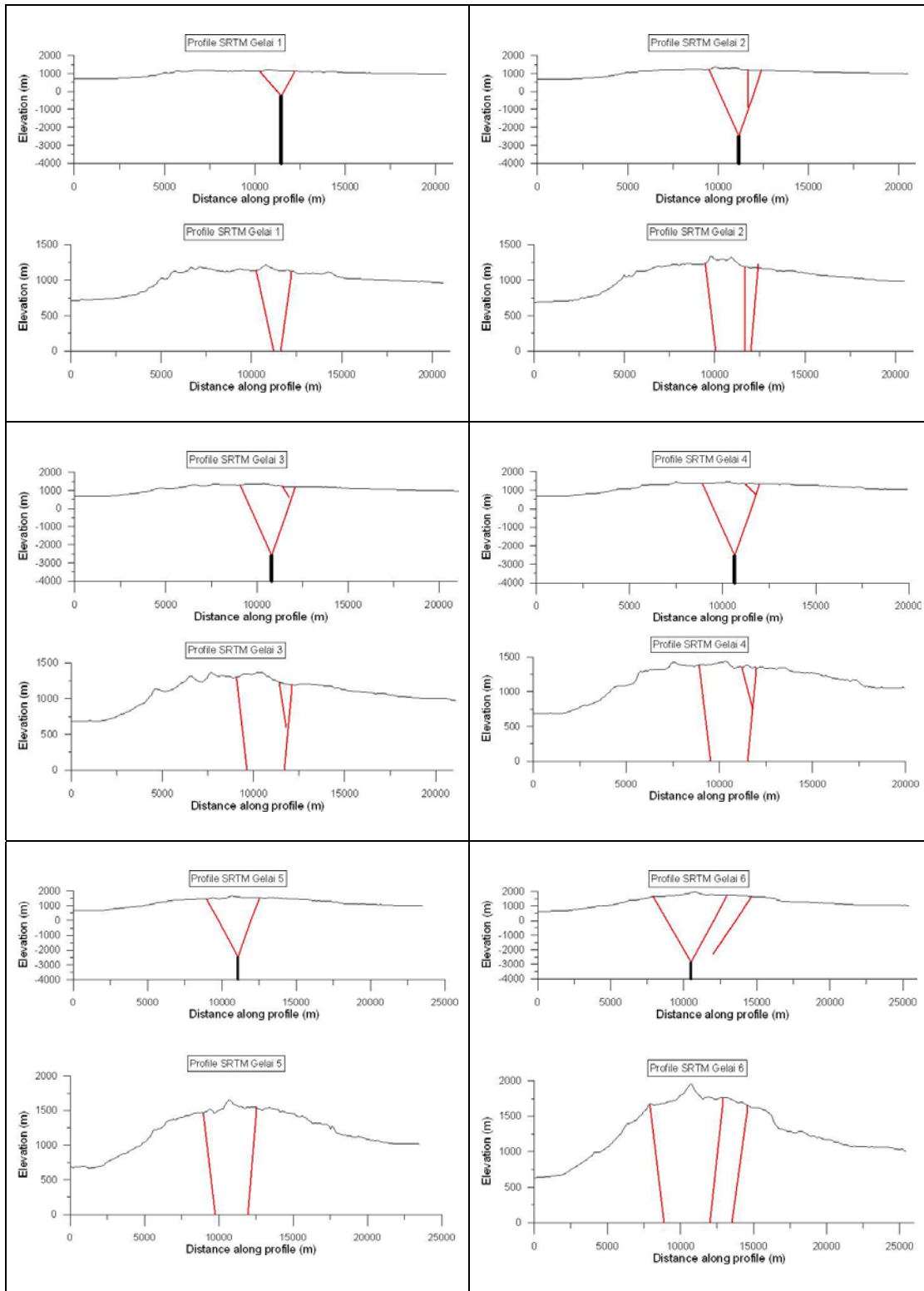


Figure 12. Topographic profiles derived from the SRTM-DEM (90 m resolution) across the Gelai tectono - magmatic graben (location on Figure 13) illustrating the calculation of the position (elevation and distance along profile) of the intersection between the two normal faults bounding the graben. This point of intersection is assumed to be close to the top of the inferred underlying dike as detailed in Figure 10. For each profile, the upper figure shows the structure at the true scale, and the lower figure, with a vertical exaggeration.

The upward projection of the top of dike is shown on Figure 14. It forms a slightly but regularly curved line on plan view when using the first solution for Profile 5 (with the western normal fault dipping  $65^\circ$  to the East). This solution is also giving the shallowest depth for the top of dike (-2067 m a.s.l.), higher than the average level found along profiles 1 to 3 (-2480 to -2580 m). The last solution for Profile 5 ( $70^\circ$  dip) gives a deeper level for the top of dike (-2480 m), in alignment with the results obtained for profiles 1 to 3. However, the geographic coordinates of the top of the dike are shifted along the profiles to the SE, giving a broken line aspect to the map projection of the top of dike. Therefore, we prefer the first solution with a dip angle of  $65^\circ$  to respect the overall curvature of the dike in plan view.

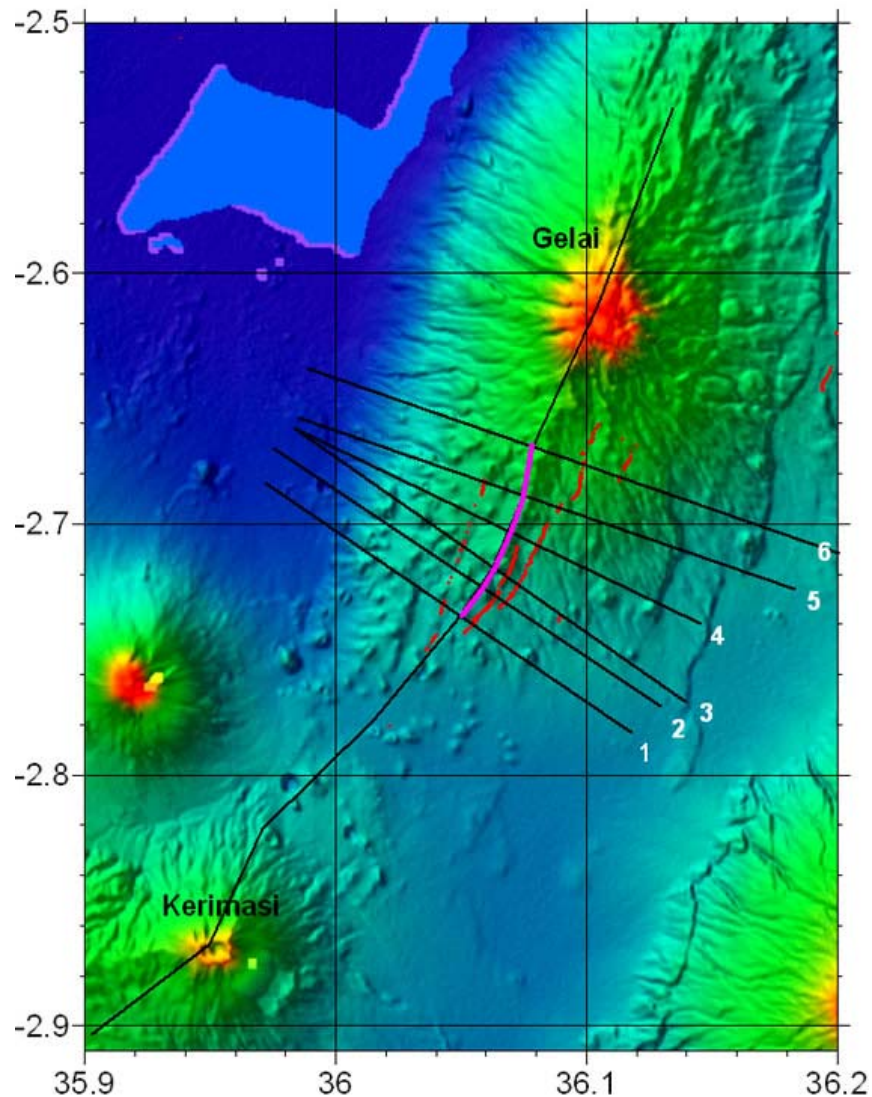


Figure 13. Location of the transversal and longitudinal profiles extracted from the SRTM-DEM (shown as artificially shaded, color - coded image). Geodetic coordinates in degrees, WGS84 datum:  $0.1^\circ$  corresponding to 9 km.

A longitudinal profile extracted from the SRTM DEM data passing through the calculated dike coordinates and the summits of both the Kerimasi and Gelai volcano (Figure 13) is shown of Figure 14. For profiles 2 to 6, the inferred top of dike is fluctuating between -2840 m a.s.l., 4750 m under the topographic surface, profile 6 and -2070 m a.s.l. or 3700 m under the topographic surface (5), with an average elevation close to -2500 m a.s.l.

Note: The observed fluctuation of the elevation of the top of dike cannot be considered as significant, due to the limited accuracy of the values (Accuracy still to be calculated).

At the level of profile 1, the calculated top of dike is significantly higher, reaching -3m a.s.l., 1747 m under the topographic surface. This corresponds to the narrower part of the graben, between the Western fault and the E1 fault. It should be noted that to other profiles (2-6), the depth of the top of dike is constrained on the eastern side of the graben, by the E2 fault instead of the E1 fault as for profile 1. In spite of this shift, the geometry of the top of dike still follows a nice curve in plan view, suggesting that the dike has been injected to a higher level, but along a similar planed (assumed vertical).

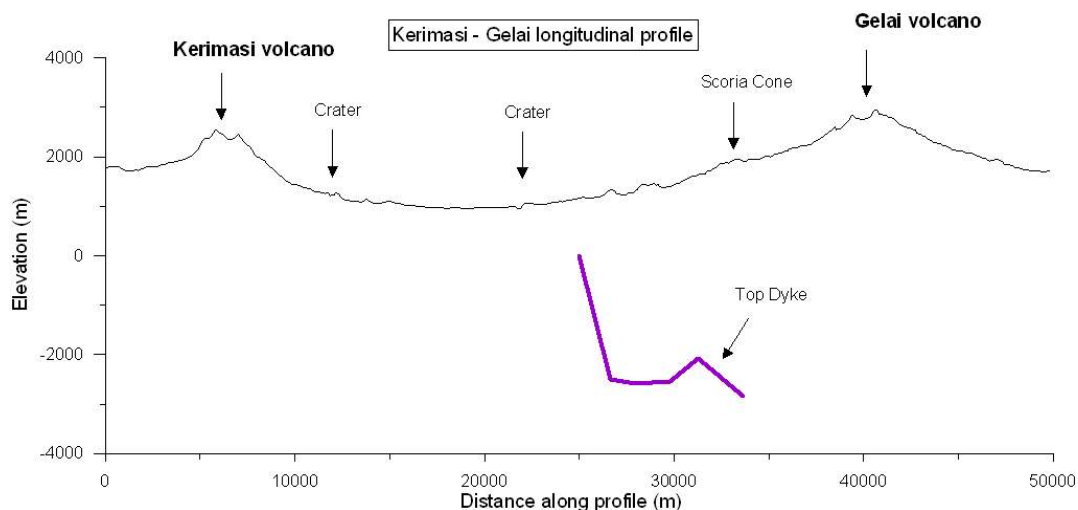


Figure 14. Longitudinal topographic profile extracted from the SRTM - DEM at 90-m resolution, passing through the surface projection of the mapped top of dike.

The surface projection of the mapped dike corresponds to several volcanic vents as seen on the referenced geological map (Figure 15). The calculated depth for the top of dike along profile 1 suggests also that the magmatic injection at the southern extremity of the dike is approaching the surface, in the vicinity of the crater that marks the southern termination of the graben system, and corresponds to the lateral intersection of the two fracture systems. However, at the present case, magma has not reached the surface though it is most likely that in the past the magma reached the surface.

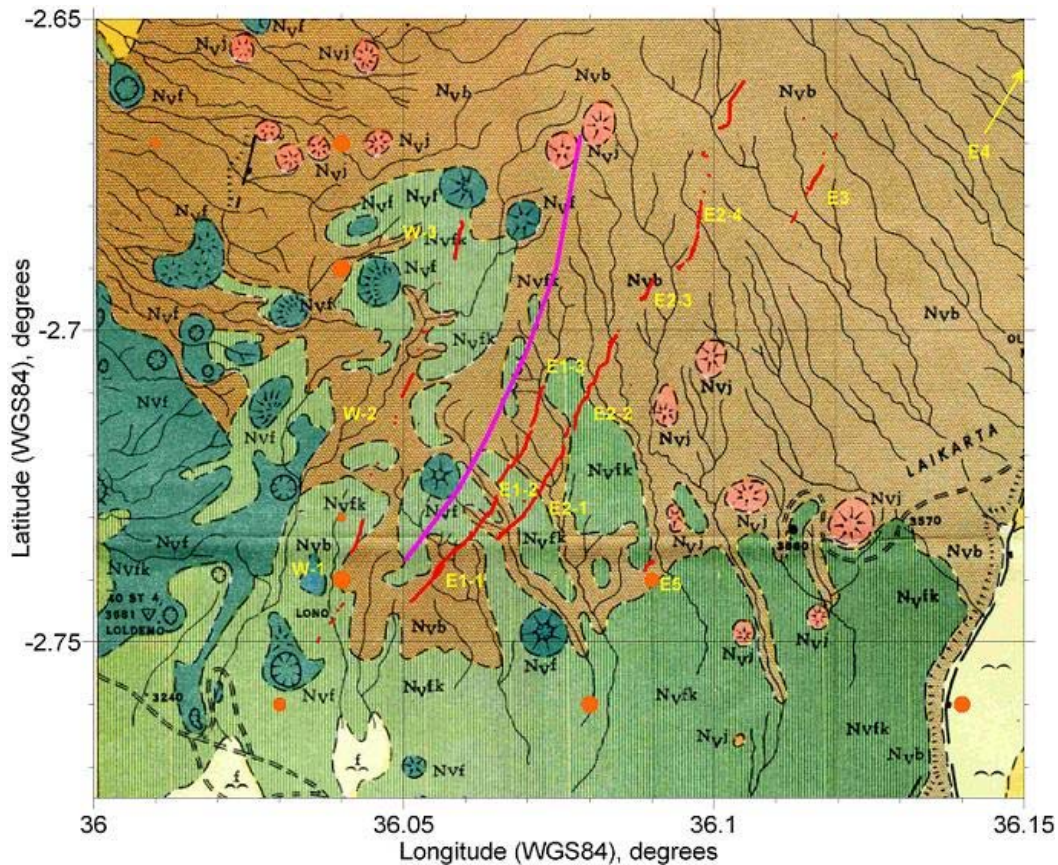


Figure 15: Plot of the fracture system (red lines and dots) and the surface projection of the calculated top of dike (violet) with the geo-referenced 1/250.000 geological map (QDS 40-1 Gelai) as the background. The volcanic vents are indicated as Nvj (“recent” scoria cones) and Nvf (“Older” Tuff and agglomerate craters).

Figures 16 and 17 display another representation of the calculated dike, assumed vertical.

### **Summary and discussion**

In summary, the field mapping of the surface fractures that appeared during the July - August volcano - seismic Gelai crisis confirms the preliminary interpretation of the SAR interferograms and provides structural and deformation data that allow to reconstruct at depth, the geometry of the top of the magmatic dike which we believed is responsible for the observed surface fractures.

The geometry of the top of dike manifests itself as a regular curved line in plan view but with irregular elevation in vertical longitudinal section. This suggests that the injection of the magma occurred along a (sub) vertical plane, curved in plan - view.

Field data show that this event is not unique in the local geological history as signs for repeated activation during the past were observed.

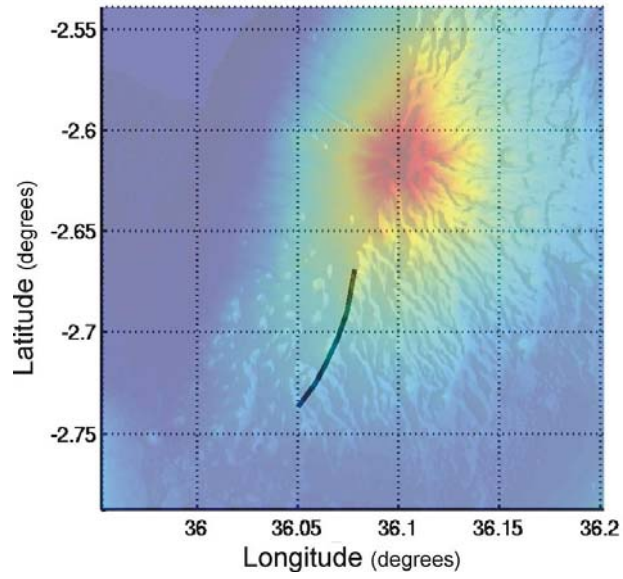


Figure 16

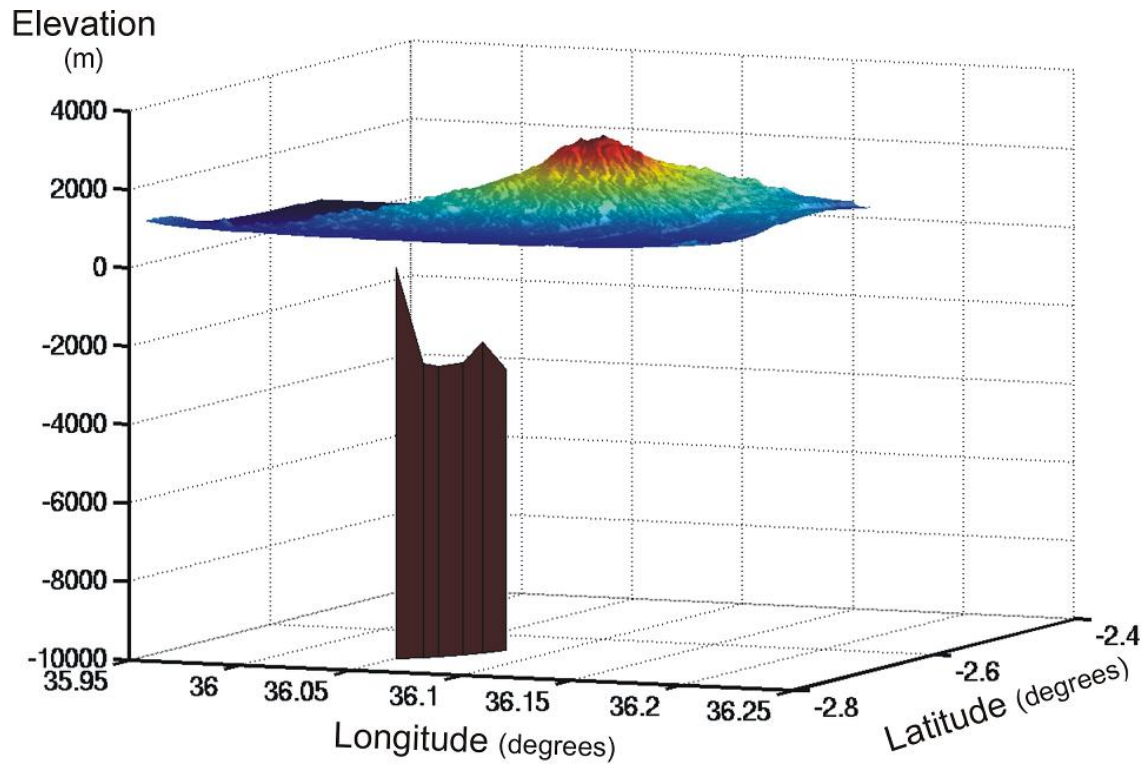


Figure 17

---

## **Acknowledgements**

The Ministry of Land Survey and the Department of Geomatics of the ARDHI University of Dar es Salaam (formerly UCLAS) are thanked for their help in organising the field campaign. E. Sariah (ARDHI) and A.S. Macheyeke (Madini Institute, Dodoma) assisted us in the field.

## **References:**

- Angelier, J., Bergerat, F., Dauteuil, O., Villemin, T. 1997. Effective tension-shear relationships in extensional fissure swarms, axial rift zone of northeastern Iceland, *Journal of Structural Geology*, 19 (5): 673-685.
- Hackett, W.R., Jackson, S.M. and Smith, R.P.. Paleoseismology of volcanic environments. In: McCaillin, J., 1996. Paleoseismology. Academic Press. San Diego, 588p.